Intelligent Cooperative Manipulation Using Dynamic Force Simulator

Martin BUSS Hideki HASHIMOTO

Institute of Industrial Science, University of Tokyo
7-22-1 Roppongi, Minato-ku, Tokyo 106, Japan
Tel +81-3-3402-6231 Ext 2359/2360 Fax +81-3-3423-1484
E-mail: martin@ics.iis.u-tokyo.ac.jp

Abstract

Intelligent Cooperative Manipulation is proposed as a new paradigm for human-machine interaction and cooperation. Aiming at intelligent assistance of human operators the information and power flow between operator—system—task environment is carefully analyzed using a virtual reality to simulate the task environment. Central issue of this virtual reality is the in this paper proposed Dynamic Force Simulator (DFS) for feedback force calculation. The DFS simulates object dynamics, contact model and friction characteristics of the human hand interacting with objects in the virtual reality. After derivation of kinematic and force relations between hand and object space we propose a method for calculation and feedback of appropriate forces to the force controlled actuators of the sensor glove we have developed. A numerical simulation example showing the efficiency of the proposed realization scheme of the DFS concludes the paper.

1 Introduction

As a step to human friendly technical systems we have proposed the Intelligent Assisting System – IAS, which assists human operators performing mechanical manipulations in the task environment[2][3]. To influence the environment state physical actions must be exerted on objects, which we call flow of power. Of course flow of information is equally important, but only the combination comes close to what humans do everyday in their environment.

The idea of the IAS considers these information and power flows and aims at physical manipulation assistance as a first step. Information flow means various data from sensors, task goals, etc. and power flow consists of forces and work between operator, the IAS and the task environment. In the following information and power flow is abbreviated as IP-flow.

As a first approach to realization of the IAS we are developing a Skill Acquisition and Transfer System including a force feedback sensor glove device and virtual world graphics animation interface. Central issue for realistic force feedback to the human operator is the Dynamic Force Simulator DFS proposed in this paper.

Research in artificial world and human-machine interfaces has so far concentrated on high-quality graphics animation and was less concerned about force feedback. The development of effective force feedback devices is just in the beginning phase, where some rather sophisticated devices have emerged[1][8][13]. We strongly think that an easy to use human-machine interface has to include some force exchange too.

In Section 2 of this paper a general description of the idea of human-machine cooperative manipulation is given. Considering 3 IP-flows (skill acquisition, skill transfer and cooperative manipulation) this systems aims at analysis and data base acquisition of the performed manipulation skill. Section 3 derives the method for realization of the Dynamic Force Simulator—DFS which calculates appropriate feedback forces as a result of sensor glove and virtual object interaction.

2 ICMS—Intelligent Cooperative Manipulation System

2.1 Functional Description

As a first approach to realization of the IAS we have been developing a skill acquisition and transfer system consisting of a sensor glove device for force feedback to the human operator, and a virtual reality including a Dynamic Force Simulator (DFS) which calculates the feedback forces to the operator. Most important characteristics of this system are the 3 information and power flows as illustrated in Fig. 1.

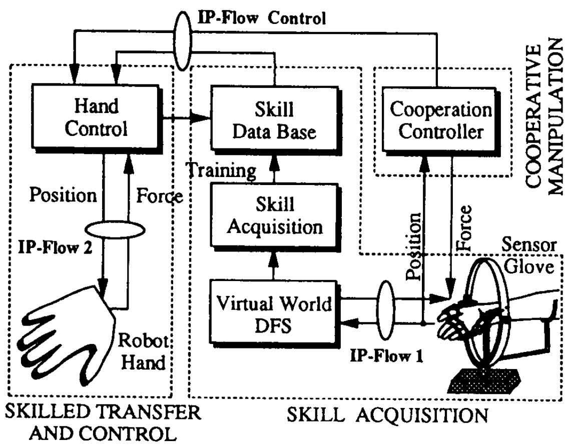

Figure 1: Intelligent Cooperative Manipulation System—ICMS.

IP-Flow 1—Skill Acquisition: The human operator wears a sensor glove device enabling interaction with objects in the virtual world while getting appropriate force feedback from the DFS. Visual feedback information from the virtual world graphic animation module is utilized by the operator for task goal verification and overall environment perception. Such visual information is important to humans for efficient manipulation planning. Force feedback is necessary for efficient manipulation control during contact between hand and object.

Analyzing the available data of joint torques and positions, essential parameters for the model of the performed manipulation skill can be derived, which are stored in the skill data base.

IP-Flow 2—Skill Transfer: The acquired skill now available in the skill data base is used for intelligent control of a robotic hand. Information from visual, tactile and joint torque sensors is used by the hand controller the same way the human did during skill acquisition. Based on this sensory information and the task goal the hand controller selects an appropriate skill from the data base selecting a control algorithm for the hand actuators exerting power on the environment. Since only essential parameters are stored in the data base, the robot hand not necessarily needs to have the same structure as the sensor glove used for skill acquisition.

IP-Flow 3—Assisting Manipulation: This is the most complex IP-flow, where the system performs as an IAS for human operator assistance. We have simultaneous IP-flow between human operator⇔DFS and skill data base⇔executing robotic hand. The *assistant* function block supervises control of this IP-flow, identifies and anticipates the action the human operator wants to perform, and if the necessary skill has been stored in the skill data base before, it is applied. In case of unknown tasks, the assistant automatically switches in acquisition mode, learning new manipulation skills on-line.

Using a data base to accumulate manipulation skills has a number of advantages over directly coupled teleoperation systems. For example the actions on the operator can be executed at a different time and location. Further, since different kinematic structures are to be considered, virtually any kinematic structure of the executing robotic hand can be controlled to manipulate objects in differently scaled macro- or micro-environments.

2.2 Experimental System

For real-time graphics animation a Silicon Graphics IRIS workstation is used displaying the state of the hand and object in the virtual world at a frame rate of 30 frames per second. A SPARC II workstation calibrates the sensor

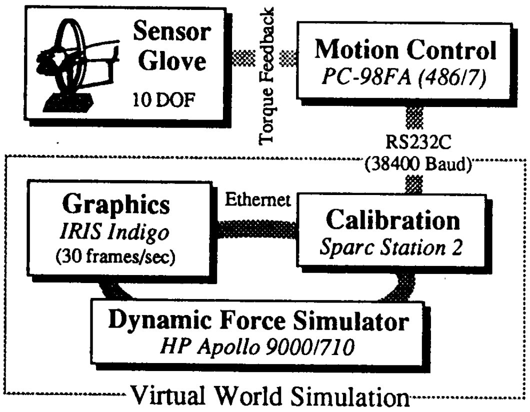

Figure 2: Virtual World Simulator and DFS.

glove joint angles using an Artificial Neural Network approach[5][6]. The overall network of these computing resources enables parallel processing of graphics, DFS calculations, motion control and sensor glove calibration in real-time.

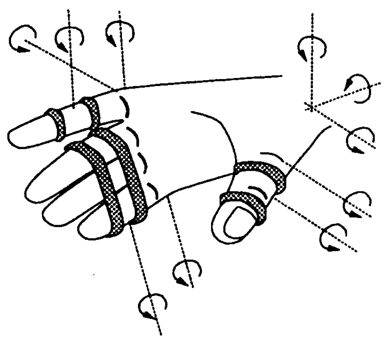

Figure 3: Schematic of Sensor Glove Structure.

The sensor glove device we have developed has 10 degrees-of-freedom, 3 degrees of freedom for the wrist, 3 for the index finger, 2 for the thumb and 2 for the rest of the fingers. In this paper we propose a method for realization of the DFS with detailed derivation of the information and power flows during interaction of the human operator and objects in the virtual environment. The experimental system structure of the DFS is shown in Figure 2.

3 Dynamic Force Simulator—DFS

While manipulating an object the generalized external force $\boldsymbol{f}_{ext} \in \mathcal{R}^6$ interacts with forces $\boldsymbol{f}_i$ from the fingers in contact with the object(Fig.5). The object is moved by the force $\boldsymbol{f}_o$ (gravity and the inertia force) and the force $\boldsymbol{f}_h$ exerted by the hand. After balancing $\boldsymbol{f}_o - \boldsymbol{f}_h$ the remainder is fed back to the human hand yielding force perception or acts on the object as an acceleration force.

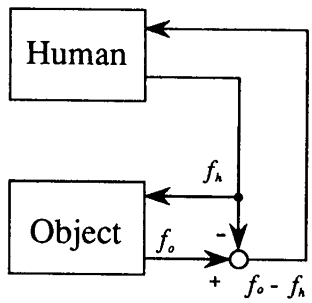

Figure 4: Relation between Human and Object.

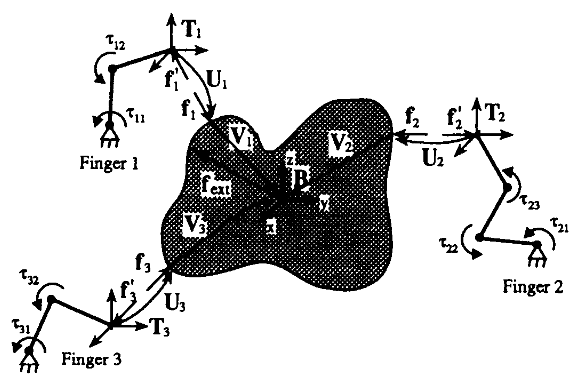

Figure 5: Object Grasped by 3 Fingers.

3.1 Coordinate Transformations Between Hand and Object

Figure 5 illustrates the transformations between finger-tip, contact and object coordinate frames. Let us define transformation matrices $\boldsymbol{U}_i \in \mathcal{R}^{4\times4}$ and $\boldsymbol{V}_i \in \mathcal{R}^{4\times4}$, where $\boldsymbol{U}_i$ transforms from the finger-tip coordinate frame $\boldsymbol{T}_i$ to the contact frame $\boldsymbol{C}_i$, and $\boldsymbol{V}_i$ from the contact frame to the object frame $\boldsymbol{B}$ as

$$\boldsymbol{T}_i \xrightarrow{\boldsymbol{U}_i} \boldsymbol{C}_i \xrightarrow{\boldsymbol{V}_i} \boldsymbol{B}\ . \qquad (1)$$

The x- and y-axis of the contact coordinate frame $\boldsymbol{C}_i$ are tangents and the z-axis is perpendicular to the object surface curvature.

The transformation matrices $\boldsymbol{\Gamma}_i \in \mathcal{R}^{6\times6}$ and $\boldsymbol{\Lambda}_i \in \mathcal{R}^{6\times6}$ are defined such that $\boldsymbol{\Gamma}_i$ transforms finger-tip forces ${}^{T_i}\boldsymbol{f}_i$ into forces ${}^{C_i}\boldsymbol{f}_i$ in the contact coordinate frame and $\boldsymbol{\Lambda}_i$ transforms these to forces ${}^{B}\boldsymbol{f}_i$ in the object reference frame $\boldsymbol{B}$ as

$$ {}^{T_i}\boldsymbol{f}_i \xrightarrow{\boldsymbol{\Gamma}_i} {}^{C_i}\boldsymbol{f}_i \xrightarrow{\boldsymbol{\Lambda}_i} {}^{B}\boldsymbol{f}_i \ . \qquad (2) $$

The relations of (1) and (2) can be written as

$$ \begin{aligned} \boldsymbol{C}_i &= \boldsymbol{T}_i\,\boldsymbol{U}_i & (3)\\ \boldsymbol{B} &= \boldsymbol{C}_i\,\boldsymbol{V}_i = \boldsymbol{T}_i\,\boldsymbol{U}_i\,\boldsymbol{V}_i & (4)\\ {}^{C_i}\boldsymbol{f}_i &= \boldsymbol{\Gamma}_i\,{}^{T_i}\boldsymbol{f}_i & (5)\\ {}^{B}\boldsymbol{f}_i &= \boldsymbol{\Lambda}_i\,{}^{C_i}\boldsymbol{f}_i = \boldsymbol{\Lambda}_i\,\boldsymbol{\Gamma}_i\,{}^{T_i}\boldsymbol{f}_i\ , & (6) \end{aligned} $$

where $\boldsymbol{U}_i$ and $\boldsymbol{V}_i$ can be written as

$$ \boldsymbol{U}_i = \begin{bmatrix} \boldsymbol{n}_{u,i} & \boldsymbol{o}_{u,i} & \boldsymbol{a}_{u,i} & \boldsymbol{p}_{u,i} \\ 0 & 0 & 0 & 1 \end{bmatrix} \qquad (7) $$

$$ \boldsymbol{V}_i = \begin{bmatrix} \boldsymbol{n}_{v,i} & \boldsymbol{o}_{v,i} & \boldsymbol{a}_{v,i} & \boldsymbol{p}_{v,i} \\ 0 & 0 & 0 & 1 \end{bmatrix} \qquad (8) $$

and the coodinate transformations of forces $\boldsymbol{\Gamma}_i$ and $\boldsymbol{\Lambda}_i$ is given by (8) as

$$ \boldsymbol{\Gamma}_i = \begin{bmatrix} \boldsymbol{n}_{u,i}^T & \\ \boldsymbol{o}_{u,i}^T & 0 \\ \boldsymbol{a}_{u,i}^T & \\ (\boldsymbol{p}_{u,i}\times\boldsymbol{n}_{u,i})^T & \boldsymbol{n}_{u,i}^T \\ (\boldsymbol{p}_{u,i}\times\boldsymbol{o}_{u,i})^T & \boldsymbol{o}_{u,i}^T \\ (\boldsymbol{p}_{u,i}\times\boldsymbol{a}_{u,i})^T & \boldsymbol{a}_{u,i}^T \end{bmatrix} \qquad (9) $$

$$ \boldsymbol{\Lambda}_i = \begin{bmatrix} \boldsymbol{n}_{v,i}^T & \\ \boldsymbol{o}_{v,i}^T & 0 \\ \boldsymbol{a}_{v,i}^T & \\ (\boldsymbol{p}_{v,i}\times\boldsymbol{n}_{v,i})^T & \boldsymbol{n}_{v,i}^T \\ (\boldsymbol{p}_{v,i}\times\boldsymbol{o}_{v,i})^T & \boldsymbol{o}_{v,i}^T \\ (\boldsymbol{p}_{v,i}\times\boldsymbol{a}_{v,i})^T & \boldsymbol{a}_{v,i}^T \end{bmatrix} . \qquad (10) $$

Remark 1 *In case the origins of finger-tip frame $\boldsymbol{T}_i$ and contact frame $\boldsymbol{C}_i$ are identical, i.e. $\boldsymbol{p}_{u,i}^T = (0,0,0)^T$. We can then rewrite $\boldsymbol{U}_i$ as*

$$ \boldsymbol{U}_i = \begin{bmatrix} \boldsymbol{R}_{u,i} & 0 \\ 0 & 1 \end{bmatrix}, \qquad (11) $$

where $\boldsymbol{R}_{u,i} \in \mathcal{R}^{3\times3}$ describes the rotation between the finger-tip and contact frames. The transformation $\boldsymbol{\Gamma}_i$ then becomes

$$ \boldsymbol{\Gamma}_i = \begin{bmatrix} \boldsymbol{R}_{u,i}^T & 0 \\ 0 & \boldsymbol{R}_{u,i}^T \end{bmatrix} \qquad (12) $$

The sensor glove has two sensor outputs, the torques actuated by the human operator $\boldsymbol{\tau}_i$ and the finger joint angle values. From the joint angles finger-tip $\boldsymbol{\theta} \in \mathcal{R}^{10}$ coordinate frames $\boldsymbol{T}_i \in \mathcal{R}^{4\times4}$ (i is the finger number from 1 to 5) are calculated by forward kinematic equations and distances of the fingers from objects of the virtual world can be calculated. If fingers are in contact with the objects, the transformations $\boldsymbol{U}_i$, $\boldsymbol{V}_i$, $\boldsymbol{\Gamma}_i$ and $\boldsymbol{\Lambda}_i$ of the previous section follow immediately.

3.2 Flow from the sensor glove

The finger joint torques $\boldsymbol{\tau}_i$ of finger i are expressed as

$$ \boldsymbol{\tau}_i = (\boldsymbol{J}_i^T)({}^{T_i}\boldsymbol{f}_i)\ , \qquad (13) $$

where $(\boldsymbol{J}_i^T)$ is the Jacobian of finger i. The finger-tip forces ${}^{T_i}\boldsymbol{f}_i$ are

$$ {}^{T_i}\boldsymbol{f}_i = (\boldsymbol{J}_i^T)^{+}\boldsymbol{\tau}_i\ , \qquad (14) $$

where $(\boldsymbol{J}_i^T)^{+}$ is the generalized inverse of the Jacobian $\boldsymbol{J}_i^T$.

Contact Model: Before transformation of the contact forces into the object coordinate frame $\boldsymbol{B}$, a specific contact model has to be chosen. Table 1 shows point and soft finger contacts as examples (refer to [14] for details). According to the contact model we have a number of wrenches exertable on the object which we write as unit wrenches ${}^{C_i}\boldsymbol{w}_{i,j}$ in the contact frame $\boldsymbol{C}_i$.

The contact forces ${}^{C_i}\boldsymbol{f}_i$ of (5) can be written as a linear combination of the unit wrenches ${}^{C_i}\boldsymbol{w}_{i,j}$ and a rest force ${}^{C_i}\hat{\boldsymbol{f}}_i$ as

$$ {}^{C_i}\boldsymbol{f}_i = {}^{C_i}\hat{\boldsymbol{f}}_i + \sum_{j=1}^{p_i} c_{ij}\,{}^{C_i}\boldsymbol{w}_{ij}\ , \qquad (15) $$

where $j = 1, \ldots, k_i$, where k_i is the number of unit wrenches ${}^{C_i}\boldsymbol{w}_{i,j}$ which actually have influence on the object corresponding to the contact model.

The rest force ${}^{C_i}\hat{\boldsymbol{f}}_i$ in (15) yields acceleration of the finger-tip and therewith a change of contact configuration because it is not balanced by other grasping forces or the external force.

We define the contact wrench intensity vector $\boldsymbol{c}_h$ as

$$ \boldsymbol{c}_h = \begin{bmatrix} c_{11} & \ldots & c_{ij} \end{bmatrix} . \qquad (16) $$

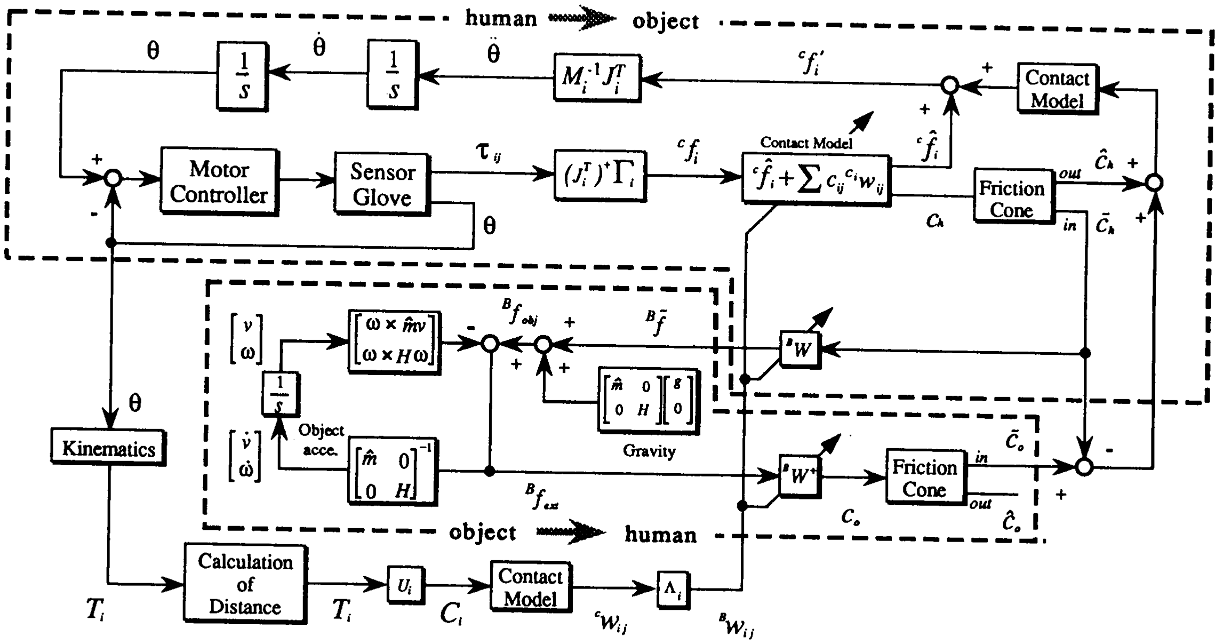

Figure 6: Dynamic Force Simulator Block Diagram.

Friction Model: If we consider a specific friction model and therewith limit the tangential component intensities $c_{i,j}$ before transformation in the object frame. For example considering Coulomb friction and a point contact model (see Table 1, the two tangential wrenches $\boldsymbol{w}_{i,1}$ and $\boldsymbol{w}_{i,2}$ are limited by the friction cone as

$$\sqrt{c_{i1}^2 + c_{i2}^2} < \mu |c_{i3}| \tag{17}$$

where μ is the Coulomb friction coefficient. The intensities $c_{i,1}$ and $c_{i,2}$ should then be limited before transformation and the remainder is included in ${}^{C_i}\hat{\boldsymbol{f}}_i$. Let us define $\boldsymbol{c}_h$ as

$$\boldsymbol{c}_h = \tilde{\boldsymbol{c}}_h + \hat{\boldsymbol{c}}_h \ , \tag{18}$$

where $\tilde{\boldsymbol{c}}_h$ is acting on the object according to the friction model and $\hat{\boldsymbol{c}}_h$ is not acting on the object.

Force not acting on the object: The force $\hat{\boldsymbol{c}}_h$ and ${}^{C_i}\hat{f}_i$ of (15) yield acceleration of the fingers. The virtual contact forces ${}^{C_i}\boldsymbol{f}_i{}'$ are

$${}^{C_i}\boldsymbol{f'}_i = {}^{C_i}\hat{\boldsymbol{f}}_i + {}^{C_i}\boldsymbol{W}\hat{\boldsymbol{c}}_h \tag{19}$$

where the contact wrench intensity $\hat{\boldsymbol{c}}_h$ is not acting on the object, the matrix ${}^{C_i}\boldsymbol{W}$ is given by the unit wrenches ${}^{C_i}\boldsymbol{w}_{i,j}$ of the chosen contact model as

$${}^{C_i}\boldsymbol{W} = \left[\ {}^{C_i}\boldsymbol{w}_{1,1} \ \ \dots \ \ {}^{C_i}\boldsymbol{w}_{i,j} \ \right] . \tag{20}$$

The finger joint accelerations $\ddot{\boldsymbol{\theta}}$ are calculated by the finger joint torques $\boldsymbol{\tau}_i$ of finger i as

$$\ddot{\boldsymbol{\theta}}_i = \boldsymbol{M}_i{}^{-1}(\boldsymbol{J}_i{}^T)({}^{C_i}\boldsymbol{f}_i') \ , \tag{21}$$

where $\boldsymbol{M}_i(\boldsymbol{\theta}_i)$ is the inertia matrix. We control the position of the motors on the sensor glove by integrating $\ddot{\boldsymbol{\theta}}$ twice to get the joint angles $\boldsymbol{\theta}$.

Force acting on the object: Assuming a contact model and therewith a unit contact wrench base the matrix ${}^B\boldsymbol{W}$ follows, which yields complete kinematic description of the transformation between hand and object space. The unit wrenches ${}^{C_i}\boldsymbol{w}_{i,j}$ are transformed into the object coordinate frame $\boldsymbol{B}$ using (5) as ${}^B\boldsymbol{w}_{i,j} = \boldsymbol{\Lambda}_i \ {}^{C_i}\boldsymbol{w}_{i,j}$ and ${}^B\boldsymbol{W}$ follows as

$${}^B\boldsymbol{W} = \left[\ {}^B\boldsymbol{w}_{1,1} \ \ \dots \ \ {}^B\boldsymbol{w}_{i,j} \ \right] \tag{22}$$

where $i = 1, \dots, n$ for n fingers and $j = 1, \dots, k_i$ for k_i wrenches exerted by finger i [10][16].

The object force ${}^B\tilde{\boldsymbol{f}}$ becomes

$${}^B\tilde{\boldsymbol{f}} = {}^B\boldsymbol{W}\tilde{\boldsymbol{c}}_h \ . \tag{23}$$

3.3 Flow from the object

Let us assume a force ${}^B\tilde{\boldsymbol{f}}$ acting on the object in the virtual world exerted by the human hand

Table 1: Contact Models

Point Contact With Friction	
twist space	wrench space
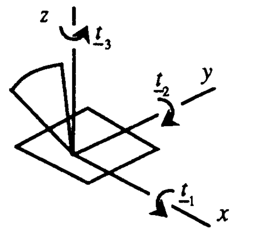	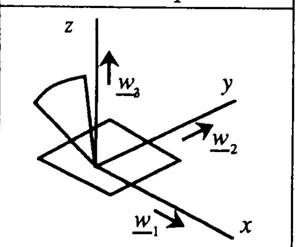
$t_1 = (0,0,0,1,0,0)^T$ $t_2 = (0,0,0,0,1,0)^T$ $t_3 = (0,0,0,0,0,1)^T$	$w_1 = (1,0,0,0,0,0)^T$ $w_2 = (0,1,0,0,0,0)^T$ $w_3 = (0,0,1,0,0,0)^T$
Soft Finger Contact	
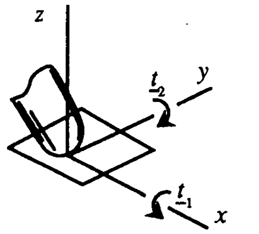	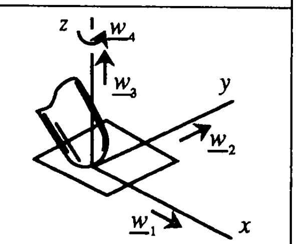
$t_1 = (0,0,0,1,0,0)^T$ $t_2 = (0,0,0,0,1,0)^T$	$w_1 = (1,0,0,0,0,0)^T$ $w_2 = (0,1,0,0,0,0)^T$ $w_3 = (0,0,1,0,0,0)^T$ $w_4 = (0,0,0,0,0,1)^T$

in the sensor glove. The object force ${}^B\boldsymbol{f}_{obj}$ is given by ${}^B\tilde{\boldsymbol{f}}$ and gravitation as

$$ {}^B\boldsymbol{f}_{obj} = {}^B\tilde{\boldsymbol{f}} + \boldsymbol{M}^* \begin{bmatrix} {}^B\boldsymbol{g} \\ \boldsymbol{0} \end{bmatrix} \quad (24) $$

where

$$ \boldsymbol{M}^* = \begin{bmatrix} \hat{\boldsymbol{m}} & \boldsymbol{0} \\ \boldsymbol{0} & \boldsymbol{H} \end{bmatrix}, $$

$\hat{\boldsymbol{m}} \in \mathcal{R}^{3\times3}$ is a diagonal matrix with the object mass in the diagonal elements, $\boldsymbol{H} \in \mathcal{R}^{3\times3}$ is the inertia matrix, ${}^B\boldsymbol{g}$ is the vector of gravitation.

Describing the object dynamics by the Newton-Euler equation as

$$ {}^B\boldsymbol{f}_{obj} = \boldsymbol{M}^* \begin{bmatrix} \dot{\boldsymbol{v}} \\ \dot{\boldsymbol{\omega}} \end{bmatrix} + \begin{bmatrix} \boldsymbol{\omega} \times \hat{\boldsymbol{m}}\boldsymbol{v} \\ \boldsymbol{\omega} \times \boldsymbol{H}\boldsymbol{\omega} \end{bmatrix} \quad (25) $$

where $\dot{\boldsymbol{v}}, \dot{\boldsymbol{\omega}}$ are the body linear and angular accelerations, the force ${}^B\tilde{\boldsymbol{f}}_{ext}$ from a object to a human is given by (24) and (25) as

$$ {}^B\boldsymbol{f}_{ext} = \boldsymbol{M}^* \begin{bmatrix} \dot{\boldsymbol{v}} \\ \dot{\boldsymbol{\omega}} \end{bmatrix} = {}^B\tilde{\boldsymbol{f}} + \boldsymbol{M}^* \begin{bmatrix} {}^B\boldsymbol{g} \\ \boldsymbol{0} \end{bmatrix} - \begin{bmatrix} \boldsymbol{\omega} \times \hat{\boldsymbol{m}}\boldsymbol{v} \\ \boldsymbol{\omega} \times \boldsymbol{H}\boldsymbol{\omega} \end{bmatrix}. \quad (26) $$

Now let us transform ${}^B\boldsymbol{f}_{ext}$ from the object frame to contact frame space using

$$ \boldsymbol{c}_o = \boldsymbol{W}^{+}\,{}^B\boldsymbol{f}_{ext}, \quad (27) $$

consider friction and therewith calculate the finger contact wrench intensities $\tilde{\boldsymbol{c}}_o$ inside the friction cone, which yields acceleration of the sensor glove finger joints.

To feedback $\tilde{\boldsymbol{c}}_o$, we have to calculate the difference between $\tilde{\boldsymbol{c}}_o$ and the finger contact wrench intensities $\tilde{\boldsymbol{c}}_h$ exerted by the human hand in the sensor glove as shown Fig.4.

The overall block diagram realizing force feed back to the sensor glove device as a result of above calculations is shown in Fig.6.

3.4 Simulation Example

Let us assume a simple example of one virtual spherical object(mass $m = 1kg$, radius $r = 0.1m$) in Fig.7. We choose a point contact model with friction. The object frame $\boldsymbol{B}$ is created as shown Fig.7 and the sphere is balanced by 4 fingers.

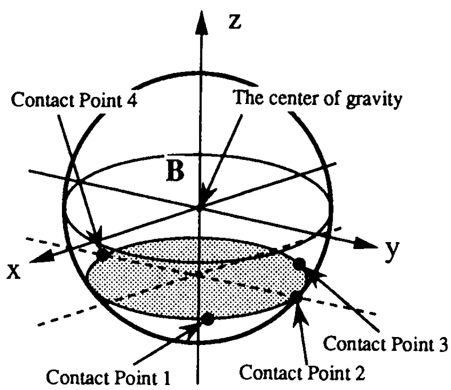

Point	Contact Point		
	x	y	z
1	0.054	0.054	-0.059
2	0	0.076	-0.059
3	-0.054	0.054	-0.059
4	0	-0.076	-0.059

Figure 7: Virtual Object and Contact Points.

In the first place, we do not add any kinds of forces on the object. Calculate the force ${}^{C_i}\boldsymbol{f}_i{}'$ from the object. The force acting on the object is only gravitation as

$$ {}^B\boldsymbol{f}_{ext}{}^T = (0 \;\; 0 \;\; -9.810 \;\; 0 \;\; 0 \;\; 0) $$

c_o is calculated by (27). All of c_o is acting on the object by friction, i.e. $\tilde{c_o} = c_o$, $\hat{c_o} = 0$. The force ${}^{C_i}f_i{}'$ acting on the finger-tip is given as

$$
\begin{aligned}
{}^{C_1}f_1{}' &= (-1.384 \;\; 0.693 \;\; 1.206 \;\; 0 \;\; 0 \;\; 0) \\
{}^{C_2}f_2{}' &= (0 \;\; -1.227 \;\; 0.956 \;\; 0 \;\; 0 \;\; 0) \\
{}^{C_3}f_3{}' &= (-1.384 \;\; -0.693 \;\; 1.206 \;\; 0 \;\; 0 \;\; 0) \\
{}^{C_4}f_4{}' &= (0 \;\; 3.415 \;\; 2.662 \;\; 0 \;\; 0 \;\; 0) \,.
\end{aligned}
$$

Using (23) and adding all ${}^{C_i}f_i'$ yields

$$ {}^{B}\tilde{f}^{T} = (0 \;\; 0 \;\; 9.81 \;\; 0 \;\; 0 \;\; 0) \,. $$

Therefore, the forces ${}^{C_i}f_i$ exerted by the operator's fingers balance gravitation acting on the object. Let us now assume that ${}^{C_i}f_i$ is 1.5 times larger than above, which yields

$$ {}^{B}\tilde{f}^{T} = (0 \;\; 0 \;\; 14.715 \;\; 0 \;\; 0 \;\; 0) \,, $$

and then

$$ {}^{B}f_{ext}{}^{T} = (0 \;\; 0 \;\; 4.905 \;\; 0 \;\; 0 \;\; 0) \,. $$

The object is accelerated by half of the gravitational force. The human operator can feel the gravitation because the force ${}^{C_i}f_i{}'$ from the object equal the first ${}^{C_i}f_i{}'$.

4 Conclusion

In this paper we proposed a new paradigm for human-machine cooperative work as in the Intelligent Cooperative Manipulation System—ICMS including a Dynamic Force Simulator (DFS) for force feedback to the human operator. Exact simulation of object dynamics, contact model and friction characteristics enables realistic feedback to the human operator. In this paper, we showed two influencing flows, the first one from human operator's hand in the sensor glove, and the second one from the solid state model of the DFS to the human hand.

Future work will include methods like efficient object modeling and data base construction describing the virtual world environment.

Acknowledgment

The authors would like to thank Mr. Koji Mukai and Mr. Nobuei Okamoto for their extraordinary support during the development of the sensor glove experimental system, Mr. Yasuharu Kunii for developing essential parts of the Dynamic Force Simulator, and Prof. Fumio Harashima for many valuable discussions and his constant encouragement.

This research was partly supported by the Electro Mechanic Technical Advancing Foundation (EMTAF) and the Japanese Ministry of Education.

References

[1] Bejczy, A.K., Teleoperation: The Language of the Human Hand, *IEEE International Workshop on Robot and Human Communication ROMAN'92*, pp.32-43, 1992.

[2] Buss, M., Hashimoto, H., Information and Power Flow During Skill Acquisition for the Intelligent Assisting System—IAS, *Proceedings of the International Workshop on Intelligent Robots and Systems IROS'93*, pp..

[3] Buss, M., Hashimoto, H., Human Manipulation Skill Analysis and Acquisition for the Intelligent Assisting System, *Proceedings of the International Federation of Automatic Control*, 1993.

[4] Cole, A., Hsu, P., Sastry, S.S., 1992. Dynamic Control of Sliding by Robot Hands for Regrasping. *IEEE Transactions on Robotics and Automation*, Vol.8, No.1, February 1992, pp.42-52.

[5] Hashimoto, H., Buss, M., Skill Acquisition for the Intelligent Assisting System Using Virtual Reality Simulator, The 2nd International Conference on Artificial Reality and Tele-Existance ICAT'92, pp.37-46, 1992.

[6] Hashimoto, H., Buss, M., Analysis and Synthesis of Human Skill for Intelligent Assisting System, *IEEE International Workshop on Robot and Human Communication ROMAN'92*, pp.177-182 , 1992.

[7] Hashimoto, H., Buss, M., Dextrous Sensor Hand for the Intelligent Assisting

System—IAS, Korean Control Conference KACC'92, pp.124-129, 1992.

[8] Iwata, H., 1990. Artificial Reality with Force-feedback: Development of Desktop Virtual Space with Compact Master Manipulator. *Computer Graphics*, Vol.24, No.4, pp.59-64.

[9] Kazerooni, H., Human-Robot Interaction via the Transfer of Power and Information Signals, *IEEE Transaction on Systems, Man and Cybernetics*, Vol.20, No.2, March/April 1990, pp.450-463.

[10] Kerr, J. and Roth, B., 1986. Analysis of Multifingered Hands. *International Journal of Robotics Research*, Vol.4, No.4, 1986, pp.3-17.

[11] Kobayashi, H., 1985. Control and Geometrical Considerations for an Articulated Robot Hand. *International Journal of Robotics Research*, Vol.4, No.1, Spring 1985, pp.3-12.

[12] Li, Z., Sastry, S.S., 1988. Task-Oriented Optimal Grasping by Multifingered Robot Hands. *IEEE Journal of Robotics and Automation*, Vol.4, No.1, February 1988, pp.32-44.

[13] Marcus, B., Feedback Technology and Virtual Environments, The 2nd International Conference on Artificial Reality and Tele-Existence ICAT'92, pp.87-95, 1992.

[14] Mason, M.T., Salisbury, J.K., 1985. Robot Hands and the Mechanics of Manipulation. *MIT Press*, Cambridge, Massachusetts, 1985.

[15] Paul, R.P., 1982. Robot Manipulators: Mathematics, Programming and Control. *The MIT Press.*

[16] Salisbury, J.K. and Craig, J.J., 1982. Articulated Hands: Force Control and Kinematic Issues. *International Journal of Robotics Research*, Vol.1, No.1, Spring 1982, pp.4-17.

[17] Yoshikawa, T., Nagai, K., 1988. Evaluation and Determination of Grasping Forces for Multi-Fingered Hands. *Proceedings of the 1988 IEEE International Conference on Robotics and Automation*, pp.245-251.

[18] Yoshikawa, T., Zheng, X., 1991. Coordinated Dynamic Control for Multiple Robotic Mechanisms Handling an Object. *Proceedings of the International Workshop on Intelligent Robots and Systems IROS'91*, pp.315-320.